JPET Fast Forward. Published on September 13, 2011 as DOI: 10.1124/jpet.111.185678

JPET #185678

Impact of Pyrrolidine Dithiocarbamate and Interleukin-6 on mTOR Complex 1 Regulation and Global Protein Translation

Shaoming Song, Kotb Abdelmohsen, Yongqing Zhang, Kevin G. Becker, Myriam Gorospe, and Michel Bernier

Laboratory of Clinical Investigation (SS, MB), National Institute on Aging, National Institutes of Health, Baltimore, Maryland 21224; Laboratory of Molecular Biology and Immunology (KA, MG), National Institute on Aging, National Institutes of Health, Baltimore, Maryland 21224; Gene Expression and Genomics Unit (YZ, KGB), Research Resources Branch, National Institute on Aging, National Institutes of Health, Baltimore, Maryland 21224.

Running Title: Divergent Regulation of mTOR complex 1 by PDTC and IL-6

Corresponding Author: Michel Bernier, Ph.D., Laboratory of Clinical Investigation, National Institute on Aging, National Institutes of Health, Biomedical Research Center, 251 Bayview Boulevard, Suite 100, Baltimore, Maryland 21224. Phone: 410-558-8199; FAX: 410-558-8381; E-mail: Bernierm@mail.nih.gov

Number of text pages: 20 (Title page -> acknowledgments)

Number of Tables: 3

Number of Figures: 4

Number of references: 40

Abstract: 242 words

Introduction: 694 words

Discussion: 1441 words

List of nonstandard abbreviations: PDTC, pyrrolidine dithiocarbamate; NF-κB, nuclear factor kappa B; HSF1, heat shock factor 1; IL-6, interleukin 6; STAT3, signal transducer and activator of transcription-3; PI3K, phosphatidylinositol 3-kinase; ERK, extracellular signal-regulated kinase; mTOR, mammalian target of rapamycin; mTORC1, mTOR complex 1; fdr, false discovery rate; PCA, principal component analysis; TSC, tuberous sclerosis complex; mTORC2, mTOR complex 2; IRES, internal ribosome entry site.

Recommended section assignment: Cellular and Molecular

Abstract

Interleukin-6 (IL-6) is a proinflammatory cytokine that exerts a wide range of cellular, physiological and pathophysiological responses. Pyrrolidine dithiocarbamate (PDTC) antagonizes the cellular responsiveness to IL-6 through impairment in STAT3 activation and downstream signaling. In order to further elucidate the biological properties of PDTC, global gene expression profiling of human HepG2 hepatocellular carcinoma cells was carried out after treatment with PDTC or IL-6 for up to 8 h. Through an unbiased pathway analysis method, gene array analysis showed dramatic and temporal differences in expression changes in response to PDTC vs. IL-6. A significant number of genes associated with metabolic pathways, inflammation, translation and mitochondrial function were changed, with ribosomal protein genes and DDIT4 primarily up-regulated with PDTC but down-regulated with IL-6. Quantitative PCR and Western blot analyses validated the microarray data and showed the reciprocal expression pattern of the mTOR negative regulator, DDIT4, in response to PDTC vs. IL-6. Administration of PDTC resulted in a rapid and sustained activation of Akt, and subsequently blocked the IL-6-mediated increase in mTOR complex 1 function through upregulation in DDIT4 expression. Conversely, the reduction in IL-6-dependent mTOR activation by PDTC was dampened in *DDIT4*-knockdown cells**.** The overall protein biosynthetic capacity of the cells was severely blunted by IL-6 but increased in a rapamycin-independent pathway by PDTC. These results demonstrate a critical effect of PDTC on mTOR complex 1 function and provide evidence that PDTC can reverse IL-6-related signaling via induction of DDIT4.

Introduction

Pyrrolidine dithiocarbamate (PDTC) is a clinically tolerated small thiol compound with antioxidant and antiinflammatory properties (Chabicovsky et al., 2010). It has been recently suggested that PDTC prevents dyslipidemia and renal lesions in rats fed a high–fat diet, most likely due to attenuation of pro-inflammatory gene expression and improvement of metabolic parameters (Ebenezer et al., 2009). Glucose-stimulated insulin secretion in human islets exposed to high glucose is restored after exposure to PDTC (Maedler et al., 2002). Furthermore, PDTC provides neuroprotection in hypoxic-ischemic injury and against liver injury during intestinal ischemia and reperfusion in rats (Nurmi et al., 2006; Tian et al., 2006). Although some studies have suggested that PDTC significantly reduces inflammatory processes through inhibition of the transcription factor nuclear factor-kappa B (NF-κB) (Schreck et al., 1992; Cuzzocrea et al., 2002; Ebenezer et al., 2009), this has not been observed in all studies (Malm et al., 2007; Huang et al., 2008). In fact, PDTC confers adaptive protection of stressed cells from pro-inflammatory conditions through activation of metal-activated transcription factor heat shock factor 1 (HSF1) (Song et al., 2010). Moreover, PDTC is a potent inhibitor of interleukin (IL)-6 transcriptional activity, thereby leading to decreased synthesis of type II acute-phase proteins in the human HepG2 hepatocellular carcinoma cell line (He et al., 2006; Xie et al., 2009). Collectively, these studies suggest that PDTC is a potent pharmacological agent with complex biological functions in the context of inflammation and other stressors. There is, however, no comprehensive information on the effects of PDTC on global gene expression profiles and related biological processes in hepatocytes.

The pro-inflammatory role of IL-6 is initiated by binding to its cell surface receptor with subsequent activation of three canonical signaling pathways (Neurath and Finotto, 2011). IL-6 activates Janus family kinases, which leads to phosphorylation of a latent pool of signal transducer and activator of transcription-3 (STAT3) at Tyr705, promoting its nuclear translocation, DNA binding and subsequent target gene expression. The phosphorylation of phosphoinositol 3-kinase (PI3-K) in response to IL-6 results in Akt activation and, hence, crosstalks with growth factor signaling pathways. In addition, IL-6 also activates

the pro-oncogenic Ras/Raf/Mek/Extracellular signal-Regulated Kinase (Erk) 1/2 signaling pathway. Given the notion that inflammation may serve as a precursor to many human diseases (e.g., cancer and type 2 diabetes), it is likely that down-modulation in IL-6 signaling pathway may have therapeutic value against pathological inflammatory conditions.

Our recent work clearly established that treatment of HepG2 cells with PDTC elicits rapid change in the expression of stress-related genes through up-regulation of the HSF1 transcription factor (Song et al., 2010). In that study, it was found that genes encoding molecular chaperones and co-chaperones were activated rapidly in response to PDTC (within 1-4 h) and that the corresponding transcripts were made soon after following stimulation by PDTC. Here, we opted to carry out gene profiling to gain insight into the nature of the genes that were modulated transiently and rapidly (up to 8 h) in response to PDTC vs. IL-6, as many of these genes will likely encode transcription factors and coregulators, secreted proteins, enzymes and other proteins involved in early regulation of cellular homeostasis. We report that PDTC time-dependently induced significant and qualitative changes in gene expression that were remarkably different to the effect of IL-6 in HepG2 cells. PDTC was found to inhibit the IL-6-dependent increase in mTOR complex 1 (mTORC1) activity by preventing the reduction in the expression of DDIT4, a negative regulator of the mammalian target of rapamycin (mTOR). The negative regulation of mTORC1 involves the binding of DDIT4 to 14-3-3 and the subsequent release of the tumor suppressor, tuberous sclerosis complex2 (TSC2), which is then free to form a complex with TSC1 and attenuate mTORC1 activity (DeYoung et al., 2008). mTORC1 plays a key role in the overall protein biosynthetic capacity (Foster and Fingar, 2010), and genes encoding ribosomal proteins and translation factors are often co-regulated to efficiently adjust the global rates of protein synthesis of the cell (Mayer and Grummt, 2006; Jastrzebski et al., 2007). Here, additional experiments showed significant differences in the pattern of expression of ribosomal protein genes and global translational activity in response to treatment with PDTC vs. IL-6.

Materials and Methods

Cell Lines. Human HepG2 (Cat. No. HB-8065) and PANC-1 (Cat. No. CRL-1469) cells were purchased from the American Type Culture Collection (Manassas, VA). HepG2 cells were maintained in MEM (Invitrogen) supplemented with 4 mM L-glutamine, 1 mM sodium pyruvate, 10% fetal bovine serum (FBS, Hyclone) and 1% penicillin-streptomycin, while PANC-1 cells were maintained in DMEM supplemented with 4.5 $g.L^{-1}$ glucose, 4 mM L-glutamine, 1 mM sodium pyruvate, 1.5 $g.L^{-1}$ sodium bicarbonate, penicillin-streptomycin and 10% FBS. All cell lines were cultured at 37 ºC under humidified 5% CO_2 in air, and the medium was replenished every three days. Cells were sub-cultured as they reached confluence.

Microarray Experiment. Serum starved HepG2 cells were left alone or incubated with either 50 µM PDTC (Sigma-Aldrich, St-Louis, MO) or 20 ng/ml recombinant human IL-6 (R&D Systems Inc., Minneapolis, MN) for 1, 2, 4 and 8 h. Total cellular RNA was extracted using RNeasy plus mini kit (Qiagen, Valencia, CA), and its quality was assessed using an Agilent BioAnalyzer (Agilent Technologies, Santa Clara, CA). Microarray analysis was performed using a human Ref-8 v2 Expression BeadChip containing 22,000 clones (Illumina, San Diego, CA). In brief, a 0.5-µg aliquot of total RNA from each sample was labeled using the Illumina TotalPrep RNA Amplification kit from Ambion (Austin, TX). After a 16-h hybridization of biotin-labeled cRNA to the beadchip, the arrays were washed, blocked, and then hybridized. Biotinylated cRNA was detected with streptavidin-Cy3 and quantitated using Illumina's BeadStation 500GX Genetic Analysis Systems scanner. Image processing and data extraction were performed using BeadStudio v15 (Illumina), and the final results were analyzed using DIANE 6.0, a spreadsheet-based microarray analysis program.

Expression Data Analysis. Z score transformation was employed to normalize the raw microarray signal fluorescent values as described previously (Cheadle et al., 2003). To calculate gene expression changes after cell treatment with PDTC or IL-6 and identify significant gene profile changes between experimental groups, Z scores were converted to Z ratios, which represent fold-like changes for each gene

and the false discovery rate (fdr). Parameterized significant analysis was completed according to the 'significance analysis of microarray' protocol (Tusher et al., 2001) with ANOVA filtering ($p \leq 0.05$). Statistical analysis was based on an increase or decrease of individual genes with Z-ratio ≥ 1.5, *P*-value ≤ 0.05, and fdr ≤ 0.30. Both microarray data have been deposited in the NCBI Gene Expression Omnibus (http://www.ncbi.nlm.nih.gov/geo/) with the accession number GSE14632. Principal Components Analysis (PCA) was performed to identify changing patterns within groups. Hierarchical clustering and k-mean clustering methods were employed to find out correlations and to distinguish patterns among various treatment groups. Ingenuity pathways analysis was used to identify biological networks with the greatest number of differentially expressed genes. For each network or pathway, probability scores were calculated using the right-tailed Fisher's exact test.

Reverse Transcription and Real-time PCR Analysis. Total RNA from cultured cells was isolated using RNeasy Mini Kit (Qiagen) and first strand cDNA was synthesized using the Omniscript Reverse Transcript kit (Qiagen). Real-time PCR reactions were carried out with the TaqMan® Gene Expression Assay system method on an ABI Prism 7300 sequence detection system (Applied Biosystems, Foster City, CA). Primer pairs used for the reactions were from Applied Biosystems (DDIT4, ID #Hs00430304_g1; GAPDH, ID #Hs99999905_m1). Relative quantitation of gene expression was performed using the threshold cycle. The mRNA levels were compared to standard curves (generated using serial RNA dilutions) and differences in mRNA expression were calculated by the $2^{-\Delta\Delta CT}$ method after normalization to GAPDH mRNA. Each analyzed sample was performed in three biological replicates and at least three reactions were used. Fidelity of the PCR was determined by melting temperature analysis.

Western Blotting. Unless otherwise indicated, cells were lysed in RIPA buffer supplemented with phosphatase and protease inhibitor cocktails (Song et al., 2010). Insoluble material was removed by centrifugation (10 000 x *g*, 20 min at 4ºC) and protein concentration in the clarified lysates was determined using the bicinchoninic acid assay (Thermo-Pierce, Rockford, IL). Proteins were separated by SDS-PAGE under reducing conditions and transferred onto polyvinylidene difluoride membranes using

JPET Fast Forward. Published on September 13, 2011 as DOI: 10.1124/jpet.111.185678
This article has not been copyedited and formatted. The final version may differ from this version.

iBlot (Invitrogen). After blocking step, membranes were probed with specific primary antibodies followed by incubation with horseradish peroxidase-conjugated secondary antibody. Visualization of immunoreactive bands was performed by enhanced chemiluminescence and quantified by volume densitometry using ImageJ software (NIH) and normalization to β-tubulin or HSP90α as loading control. The primary antibodies were directed against DDIT4 (rabbit, Proteintech group, Chicago, IL), STAT3 (rabbit, Santa Cruz Biotechnology, Santa Cruz, CA), Hsp90α (mouse, BD Biosciences); phospho-4EBP1 (Thr37/Thr46), phospho-S6K1 (Thr389), phosphoSTAT3 (Tyr705), phosphoAkt (Ser473), phosphoAkt (Thr308), phosphoTSC2 (Thr1462), phosphoGSK3β (Ser9), S6K1, Akt, and β-tubulin (1:1000; rabbit, Cell Signaling Technology, Danvers, MA).

siRNA Knockdown Experiments. The small interfering RNA (siRNA) duplex used in this study was targeted against DDIT4 (Ambion/Applied Biosystems). The sequence of the DDIT4 siRNA duplex was as followed: (sense) 5'-ACGCAUGAAUGUAAGAGUAtt-3', (antisense) 5'-UACUCUUACAUUCAUGCGUct-3'. The negative control siRNA was the "AllStars Neg. control siRNA" (Qiagen) that has no known target gene. HepG2 cells (2-3 x 10^5 cells/ml) in antibiotics-free MEM were subjected to reverse transfection using Lipofectamine RNAiMAX reagent (Invitrogen) and 20-40 nM siRNA duplex per 35-mm plate according to the supplier's instructions. Specific target gene silencing was confirmed by real-time PCR and immunoblotting 2 days after reverse transfection.

Global [^{35}S]-labeled Protein Translation Assay. Serum-starved HepG2 cells (seeded on 35-mm plates) were treated with PDTC or IL-6 as indicated in the text. After a series of washes in PBS, cells were incubated with Met/Cys-free medium for 30 min at 37ºC followed by the addition of 100 µCi ^{35}S Protein labeling mix (NEG-072; PerkinElmer NEN Radiochemicals, Waltham, MA) and further incubation for 15 min. Cells were lysed in RIPA buffer and equal amounts of proteins were loaded on SDS-polyacrylamide gels, transferred to a PVDF membrane and visualized with a PhosphorImager (Molecular Dynamics). The membrane was then reprobed for β-actin by Western blotting.

Statistical Analysis. Results are expressed as mean ± standard deviation. Statistical analysis was

performed using unpaired Student's t-test or one-way ANOVA followed by Fisher's LSD post hoc test as appropriate. A value of $P< 0.05$ was considered statistically significant. All calculations were carried out using Kaleidagraph v.4.01 (Synergy Software, Reading, PA).

JPET Fast Forward. Published on September 13, 2011 as DOI: 10.1124/jpet.111.185678
This article has not been copyedited and formatted. The final version may differ from this version.

Results

Genome-wide Comparison of Expression Profiles between HepG2 Cells Treated with PDTC and IL-6. Oligonucleotide DNA microarray analysis was performed to identify changes in gene expression following treatment of HepG2 cells with either PDTC or IL-6. PCA analysis and hierarchical clustering algorithm demonstrated that the global expression patterns of PDTC-treated groups were distinctly different from those of IL-6-treated groups over time (Supplemental Fig. 1A, B). Of the 22,000 genes and expressed sequence tags that are represented on the chip, a total of 1043, 1159, 1417 and 1601 genes were differentially expressed following PDTC addition for 1, 2, 4 and 8 h, respectively, when compared to the control group ($P \leq 0.05$). Under these experimental conditions, IL-6 treatment led to 533, 1234, 1048, and 1116 regulated genes of which 123, 244, 275, and 329 genes were shared with PDTC. A heatmap representing an abridged list of 'shared' genes showed an opposite direction of change for a number of these genes when IL-6 and PDTC treatment groups were compared (Supplemental Fig. 1C). These include RPLP1 (ribosomal protein, large, P1), IER3 (radiation-inducible immediate-early gene IEX-1) and JUND (jun D) (Supplemental Table 1). On the other hand, several genes showed a similar direction of change following cell treatment with PDTC and IL-6 (Supplemental Table 2).

Analysis of Gene Sets in HepG2 Cells Treated with PDTC and IL-6. Supervised analyses, such as parameterized analysis of gene set enrichment (Kim and Volsky, 2005), provide insight into regulated signaling pathways or biological processes as well as a list of differentially expressed genes. From the collection of more than 182 gene sets we identified sets of genes that were altered by PDTC and IL-6 over time ($P \leq 0.05$; Table 1). There were 104 and 102 gene sets whose expression was altered after 8-h treatment with PDTC and IL-6, respectively, of which 36 gene sets were shared (Table 2 and Supplemental Table 3). Of note, scatter plot analysis of the cumulative z-scores of these shared gene sets showed a reverse relationship between PDTC and IL-6 (Supplemental Fig. 1D, $R^2 = 0.6835$), with nine of the 36 enriched gene sets that were directly associated with metabolic pathways, eight with inflammation and cytokine signaling, five with mitochondrial function, and three with cancer biology. This analysis was

repeated for the 1, 2, and 4 h-time points, of which 4, 21, and 38 sets of genes were shared, respectively (Supplemental Table 4). The temporal expression of gene sets that were the most differentially regulated by PDTC or IL-6 is also depicted (Supplemental Fig. 2A). Therefore, the effects on PDTC on gene expression patterns in HepG2 cells sharply differed from that observed with IL-6.

In order to focus on conditions under which the actions of PDTC toward IL-6 signaling could be best explored, we selected the mTOR complex, a key regulator in the control of protein synthesis, mitochondrial function, and inflammation-mediated tumor development (Foster and Fingar, 2010; Ramanathan and Schreiber, 2009; Lee et al., 2007). The choice of mTOR was borne out by the fact that expression of more than fifty ribosomal protein genes was sharply reduced with IL-6 but up-regulated with PDTC after a 2-h treatment (Table 3 and Supplemental Table 5). Moreover, the mTOR-associated GO term 'translation' (GO:0006412) was one of the most affected biological processes that were reciprocally affected by PDTC and IL-6 (Supplemental Fig. 2B). Among the changed genes, there was a significant 17-fold increase in DDIT4 mRNA expression at 1 h after PDTC treatment while IL-6 elicited a ~11-fold reduction as compared to untreated cells (Fig. 1A). *DDIT4* encodes a protein transcript (DDIT4, also known as REDD1 and Rtp801) that has been identified as a negative regulator of mTOR complex 1 (Foster and Fingar, 2010). Our microarray analysis demonstrated a time-dependent return of *DDIT4* expression to almost basal levels 4-8 h after the initial stimulation with either PDTC or IL-6 (Fig. 1A).

A number of significantly changed transcripts and one not significantly changed (*HSF1*) were selected for quantitative real-time PCR validation of the microarray data. Positive validation was obtained for transcripts encoding *DDIT4* (Fig. 1B), *BAG3*, *HSPA1A*, *DEDD2*, and *MCL1* (data not shown). When compared to vehicle-treated controls, there was a 4.8 ± 1.6–fold increase in DDIT4 mRNA levels with PDTC for 1 h, but a 2.9 ± 0.3–fold reduction in IL-6-treated HepG2 cells ($P < 0.001$, Fig. 1B). The role of transcription in the observed up-regulation of *DDIT4* expression by PDTC was investigated by pre-incubating HepG2 cells with actinomycin D. Inhibition of transcription resulted in a near total suppression in both the constitutive and inducible expression of DDIT4 mRNA (Fig. 1B).

PDTC blocks IL-6 suppression of DDIT4 and associated upregulation of mTOR complex 1.

Western blot analysis indicated an increase in DDIT4 expression by PDTC within 2 h and peaked at 3-4 h (Fig. 1C) before returning to basal levels by 6 h (not shown). The low abundancy of DDIT4 protein in vehicle-treated cells made it difficult to ascertain whether DDIT4 stability can be altered by IL-6. However, the use of long-exposure films enabled the detection of DDIT4 in control cells, whose level was rapidly reduced by a 1-h treatment with IL-6 before slowly returning to control levels (Fig. 1D). PDTC is a potent inhibitor of IL-6 signaling cascade whose inactivation is associated with loss in STAT3 target gene expression (Xie et al. 2009). Here, it is apparent that changes in gene expression in response to PDTC were at the very least STAT3 independent, as no tyrosine phosphorylation of STAT3 was detectable up to 4 h (Fig. 1C, middle panel, lanes 2-5). Treatment of HepG2 cells with IL-6 under serum-free conditions elicited significant tyrosine phosphorylation of STAT3 when compared to the vehicle-treated group (Fig. 1C, middle panel, lanes 6-9 vs. lane 1). While IL-6 responsiveness vis-à-vis STAT3 phosphorylation was not affected by PDTC at the 1 h time–point, longer treatment with PDTC clearly blocked the IL-6-induced phospho-STAT3 levels at 2-4 h (Fig 1C, middle panel, lanes 10-13). Under these conditions, the ability of PDTC to stimulate DDIT4 protein expression was unchanged by the presence of IL-6 (Fig. 1C, top panel, lanes 10-13).

To measure the effect of PDTC and IL-6 on mTORC1 function, we monitored the phosphorylation of the translation regulatory protein 4E-BP1 and the 70-kDa isoform of S6K1, which are frequently used as surrogate markers of mTOR kinase activity (Wullschleger et al., 2006). Here, PDTC induced rapid Thr389 phosphorylation of S6K1 by 1 h, but continued treatment for 2-4 h led to S6K1 dephosphorylation (Fig. 2, top panel). In contrast, phosphorylation of 4E-BP1 at Thr37/46 was low and remained attenuated throughout PDTC treatment up to 4 h (second panel). When cells were treated with IL-6, maximal phosphorylation of S6K1 and 4E-BP1 was achieved by 1 h and then slowly declined thereafter. While IL-6-mediated phosphorylation of S6K1 was not affected by the co-incubation with PDTC at the 1h time point, longer treatment with PDTC elicited only modest decline in IL-6 responsiveness at 2-4 h (top panel, lanes 10-13). In contrast, the presence of PDTC resulted in marked reduction in IL-6-inducible 4E-

JPET Fast Forward. Published on September 13, 2011 as DOI: 10.1124/jpet.111.185678
This article has not been copyedited and formatted. The final version may differ from this version.

BP1 phosphorylation at the 2-4 h time points, but not at the 1-h time point (Fig. 2, second panel, lanes 10-13). Taken together, these results indicate that a latency period of 1 h is required before the onset of inhibition of IL-6-dependent mTORC1 signaling by PDTC.

Selective activation of the PI3K/Akt pathway has been found to be key to early mTORC1 activation and downstream regulation of protein synthesis (Foster and Fingar, 2010). Akt activity was assessed by measuring Akt phosphorylation levels on Thr308 and Ser473 and phosphorylation of direct downstream targets, such as GSK3β on Ser9 and TSC2 on Thr1462. Treatment of HepG2 cells with IL-6 did not affect Akt activity; however, exposure to PDTC alone or combined with IL-6 resulted in rapid and sustained phosphorylation of Akt and its downstream targets up to 4 h (Fig. 2). Thus, early activation of mTORC1 signaling by PDTC and IL-6 (1 h time point) is likely to occur through distinct mechanisms.

Then, we analyzed whether the cellular response to PDTC, IL-6 and the combination PDTC+IL-6 could be confirmed in the human pancreatic carcinoma cell line, PANC-1. The reciprocal regulation of DDIT4 protein levels by PDTC vs. IL-6 and the ability of PDTC to suppress IL-6-mediated phosphorylation of STAT3 were similar in both cancer cell types, including the latency period of 1 h before the onset of PDTC inhibition (Supplementary Fig. 3A, middle panel). Moreover, treatment of PANC-1 cells with PDTC was associated with early activation with the Akt/mTORC1 pathway up to 2 h, followed by a marked reduction in the phosphorylation of Akt and mTORC1 downstream targets, S6K1 and 4E-BP1, by 4 h (Supplementary Fig. 3B). As anticipated, this phosphorylation kinetics was in opposite direction as compared to the expression of the mTORC1 negative regulator, DDIT4 (Supplementary Fig. 3A, top panel). Exposure of PANC-1 cells to IL-6 resulted in very weak activation of the Akt/mTORC1 pathway. Altogether, these results indicated that PDTC could be an effective mTORC1 repressor by up-regulating DDIT4 in two types of cancer cell lines.

To assess the role of DDIT4 in the down-modulation of mTORC1 by PDTC at the 2-4 time points, HepG2 cells were incubated with the DDIT4 siRNA and non-silencing siRNA control for 48 h. When compared with the non-silencing control group, DDIT4 knockdown blocked the inducible expression of DDIT4 protein by 50% in response to a 2-h treatment with PDTC (Fig. 3, *upper panel*). The levels of β-

JPET Fast Forward. Published on September 13, 2011 as DOI: 10.1124/jpet.111.185678
This article has not been copyedited and formatted. The final version may differ from this version.

tubulin (Fig. 3), STAT3 and Hsp90α (data not shown) were unaffected, indicating a low probability of nonspecific silencing effects. *DDIT4* silencing resulted in the protection against PDTC-mediated decrease in Thr389 phosphorylation of S6K1 while having little or no effect on 4E-BP1 phosphorylation (Fig. 3, lane 3 vs. 7). In contrast, the ability of IL-6 to promote S6K1 and 4E-BP1 phosphorylation was unaffected by *DDIT4* knockdown (lane 2 vs. 6). As indicated earlier, treatment with PDTC dramatically attenuated IL-6-induced STAT3 activation and associated mTOR downstream signaling. Here, in cells transfected with the DDIT4 siRNA, PDTC continued to exert its suppressive effects on IL-6-mediated phosphorylation of 4E-BP1 (lane 4 vs. 8).

In light of our observation that mTORC1 activity is reciprocally regulated by PDTC and IL-6, we asked whether the expression of DDIT4 was necessary for control of the global protein translation machinery. As shown in Fig. 4A, there was clear increase in the levels of ^{35}S-labeled proteins in HepG2 cells in response to a 2-h treatment with PDTC, even in the presence of the mTORC1 inhibitor, rapamycin (Fig. 4A, denoted by *). Administration of DDIT4 siRNA had no effect on the basal and PDTC-induced increase in protein synthesis. Under these conditions, rapamycin completely inhibited insulin- and IL-6-mediated S6K1 phosphorylation at Thr389 (Fig. 4B). Of note, IL-6 sharply reduced global protein translation both in control and *DDIT4* knockdown cells, consistent with lower ribosome biogenesis and function (see results above).

Discussion

In the present study, we explored and compared the effects of PDTC with that of the pro-inflammatory cytokine IL-6 on global gene expression profiling and the overall protein biosynthetic capacity in cultured hepatoma cells. To better understand the actions of PDTC in IL-6 signaling, the combination of IL-6 and PDTC was tested vis-à-vis the regulation of DDIT4 expression and its impact on mTORC1 signaling. The novel findings of this study were 1) treatment with IL-6 vs. PDTC time-dependently induced substantial changes in gene expression patterns in HepG2 cells when compared to the untreated control groups; 2) the changes in gene set enrichment were either stimulus-specific or shared by IL-6 and PDTC, with ribosomal protein genes and DDIT4 predominantly up-regulated with PDTC but down-regulated with IL-6; 3) silencing of DDIT4 slowed the adverse effects of PDTC on IL-6-dependent mTORC1 activation; and 4) the overall protein biosynthetic capacity of HepG2 cells was severely blunted by IL-6, but increased in a rapamycin-independent pathway by PDTC.

A variety of cytoprotective pathways were activated in response to PDTC, promoting changes in gene expression that facilitate cell survival and recovery from stress. For example, PDTC activates the transcription factor HSF1 (Song et al., 2010), which mediates the heat shock response, a process that controls the expression of a conserved set of inducible heat shock proteins, their DnaJ cohorts, and a variety of co-chaperones. From our microarray data, we identified a large variety of heat shock proteins that were induced by PDTC but not IL-6. A large fraction of genes involved in amino acid metabolism, mitochondrial function, and mRNA processing showed decreased expression with PDTC, whereas the opposite effect was observed with IL-6. In specifically looking for growth arrest and cell cycle-related gene products, it was found that PDTC induces a rapid but transient increase in the levels of the mTORC1 negative regulator, DDIT4, in HepG2 cells. In contrast, IL-6 treatment sharply decreased DDIT4 expression. In addition of HepG2 cells, PDTC elicited a rapid increase in DDIT4 expression in different types of human cancer cells, including PANC-1 (Supplemental Fig. 3A) and A7 melanoma cells, and in freshly isolated human peripheral blood mononuclear cells (Song and Bernier, unpublished).

Initially described as a hypoxia-inducible gene through activation of the transcription factor HIF-1α (Shoshani et al., 2002), *DDIT4* has since been reported to be a cell stress response gene and the transcriptional target of several trans-acting factors (Lin et al., 2005). Here, we found that the *DDIT4* mRNA levels changed in opposite direction during a 1-h treatment with PDTC and IL-6 in HepG2 cells, consistent with the involvement of immediate-early genes in the regulation of *DDIT4* expression. In HL-60 cells, administration of PDTC resulted in the up-regulation of the zinc finger transcription factor EGR-1 (Della Ragione et al., 2002). Although HIF-1α and EGR-1 mRNA levels were markedly up-regulated by PDTC in HepG2 cells, these transcription factors did not participate in the induction of *DDIT4* during PDTC treatment (Song and Bernier, unpublished data). Therefore, the identification of the immediate-early genes encoding transcription factors that regulate *DDIT4* expression in response to PDTC and IL-6 will require additional studies, which are beyond the scope of this paper.

In addition to transcriptional regulation, DDIT4 is also subject to post-transcriptional and translational control. The rate of DDIT4 translation is tightly regulated and DDIT4 mRNA, like the protein, has been shown to have a very short half-life. DDIT4 mRNA translation is inhibited by microRNA binding at the 3′-untranslated region, and ectopic expression of these microRNAs correlates with tumorigenesis through down-modulation of DDIT4 mRNA levels (Hwang-Verslues et al., 2011; Pineau et al., 2010). There is a large body of work detailing one of the mechanisms by which the IL-6/STAT3 pathway promotes tumor cell survival, which includes deregulated expression of microRNAs (Meng et al., 2007). Work is underway to assess the temporal expression profiles of microRNA during PDTC and IL-6 challenge in HepG2 cells and their impact on DDIT4 mRNA regulation.

Akt-mediated TSC2 phosphorylation on Thr1462 is known to relieve the inhibitory effects of the TSC1/TSC2 complex on mTORC1 (Foster and Fingar, 2010). This Akt-dependent phosphorylation of TSC2 could explain the early activation of mTORC1 by PDTC (1-h time point). However, through increased DDIT4 protein translation (2-4 h time points), PDTC might then exert a negative feedback mechanism due to reactivation of the inhibitory tonic activity of TSC2. As IL-6 activates mTORC1

signaling independently of Akt, multisite phosphorylation of TSC2 by other signaling modules, such as the Ras/ERK module (Ma et al., 2005), might provide a mechanism that leads to mTORC1 activation by this cytokine.

PDTC has been recently shown to increase protein *S*-glutathionylation in HepG2 cells, reaching a maximum by 2 h (Wang et al., 2009). Coincidentally, a 2-h exposure with PDTC is required for the marked reduction in IL-6-mediated phosphorylation of STAT3 and activation of mTORC1. A recent study has demonstrated that the ability of PDTC to promote *S*-glutathionylation of STAT3 renders it a poor substrate for the IL-6 receptor/JAK tyrosine kinase complex (Xie et al., 2009). Therefore, the temporal effects of PDTC on both the DDIT4 expression and cellular redox may ultimately contribute to the refractoriness in IL-6 signaling.

Dysregulation in DDIT4 levels has been recently linked to several human diseases, such as liver cancer (Pineau et al., 2010), and marked increase in tumorigenicity was observed *in vivo* in *DDIT4* knockout mice (Horak et al., 2010). Induction of *DDIT4* suppresses mTOR activity and its associated trophic effect on protein synthesis in HeLa cells exposed to oxidative and endoplasmic reticulum stress (Jin et al., 2009). The connection between DDIT4 and the TSC1/TSC2-mTORC1 pathway is supported by the observation that cellular stressors have been shown to block the translational machinery through DDIT4-mediated suppression of mTORC1 activity (Corredetti et al., 2005; Sofer et al., 2005). However, we observed a striking increase in global protein translation in PDTC-treated cells but suppression with IL-6. In the latter case, defect in ribosome biogenesis in IL-6-treated cells (see above) certainly contributes to lower cellular biosynthetic capacity despite mTORC1 activation. Furthermore, mTORC1/cap-dependent translation initiation would only have a minimal role in the contribution of PDTC to the rapamycin resistant translational control of protein synthesis.

It has been recently found that mTORC2 associates with ribosomal proteins to regulate mRNA translation (Dormond et al., 2008; Kuehn et al., 2011). In addition to mTORC1-mediated cap-dependent translation, translation initiation can also occur in the middle of an mRNA via a nucleotide sequence known as internal ribosome entry site (IRES) (reviewed by Komar and Hatzoglou, 2011). The latter

process enables the recruitment of 40S ribosome in the vicinity of the initiation codon with the help of IRES trans-acting factors. It is noteworthy to mention that IRES-mediated translation has been found to occur for mRNAs encoding proteins involved in either stress protection or apoptosis (Komar and Hatzoglou, 2011). Perhaps the mTORC2/40S ribosome/IRES pathway functions as a rate limiting factor for global mRNA translational responses depending on the stimulus and cell type. Nevertheless, the mechanism by which PDTC promotes global protein translation has not been investigated further in this study.

Our results suggest that mTORC2 mediates the translational activity of PDTC because PDTC strongly increases the phosphorylation of Akt on Ser473, a recognized effector of mTORC2, whose activity can be considered to be upstream of mTORC1. TSC2-Thr1462 has been found to be a direct Akt phosphorylation target site; however, TSC2 phosphorylation on additional sites may also contribute to the stimulation of mTORC2 by PDTC. The activity of mTORC2 responds to PDTC, but how mTORC2 is regulated is unclear. Sin1 (stress-activated protein kinase-interacting protein 1) and rictor maintain mTORC2 integrity and mediates mTORC2 function (Foster and Fingar, 2010). It is possible that PDTC stimulation of mTORC2 might come from enhanced binding of rictor and Sin1 to mTOR. As alluded to earlier, PDTC may modulate also mTORC2 signaling and contribute to global protein translation through phosphorylation and inactivation of TSC2.

Significance and Potential Impact

Elevated circulating levels of IL-6 is one of many factors involves in the pathophysiology of chronic inflammatory diseases and cancer cachexia. Of note, PDTC attenuates muscle and adipose tissue loss in a cachetic mouse model and reduces IL-6 synthesis from inoculated tumor tissues (Nai et al., 2007). From this and several *in vivo* studies showing minimal genotoxicity (Chabicovsky et al., 2010), PDTC qualifies as a valuable drug candidate. However, there is much to be learned on how PDTC confers protection against IL-6-mediated reduction in ribosomal protein biogenesis and subsequent decline in global protein translation. We propose that the anti-inflammatory action of PDTC calls for the inhibition of IL-6-

induced mTORC1 activity through a mechanism involving the tumor suppressor DDIT4.

Acknowledgments

We thank William H. Wood 3rd from the Gene Expression and Genomics Unit, Research Resources Branch at NIA, for his invaluable assistance with the cDNA microarray analysis. We thank also Sutapa Kole for her expert technical assistance.

Authorship Contributions

Participated in research design: Song, Abdelmohsen, Becker, Gorospe, and Bernier

Conducted experiments: Song, and Abdelmohsen

Contributed new reagents or analytic tools: n/a

Performed data analysis: Song, Abdelmohsen, Zhang, Becker, Gorospe, and Bernier

Wrote or contributed to the writing of the manuscript: Song, Zhang, and Bernier

References

Chabicovsky M, Prieschl-Grassauer E, Seipelt J, Muster T, Szolar OH, Hebar A, and Doblhoff-Dier O (2010) Pre-clinical safety evaluation of pyrrolidine dithiocarbamate. *Basic Clin Pharmacol Toxicol* **107**: 758-767.

Cheadle C, Vawter MP, Freed WJ, and Becker KG (2003) Analysis of microarray data using Z score transformation. *J Mol Diagn* **5**: 73–81.

Corradetti MN, Inoki K, and Guan KL (2005) The stress-inducted proteins RTP801 and RTP801L are negative regulators of the mammalian target of rapamycin pathway. *J Biol Chem* **280**: 9769-9772.

Cuzzocrea S, Chatterjee PK, Mazzon E, Dugo L, Serraino I, Britti D, Mazzullo G, Caputi AP, and Thiemermann C (2002) Pyrrolidine dithiocarbamate attenuates the development of acute and chronic inflammation. *Br J Pharmacol* **135**: 496–510.

Della Ragione F, Cucciolla V, Criniti V, Indaco S, Borriello A, and Zappia V (2002) Antioxidants induce different phenotypes by a distinct modulation of signal transduction. *FEBS Lett* **532**: 289-294.

DeYoung MP, Horak P, Sofer A, Sgroi D, and Ellisen LW (2008) Hypoxia regulates TSC1/2-mTOR signaling and tumor suppression through REDD1-mediated 14-3-3 shuttling. *Genes Dev* **22**: 239-251.

Dormond O, Contreras AG, Meijer E, Datta D, Flynn E, Pal S, and Briscoe DM (2008) CD40-induced signaling in human endothelial cells results in mTORC2- and Akt-dependent expression of vascular endothelial growth factor in vitro and in vivo. *J Immunol* **181**: 8088-8095.

Ebenezer PJ, Mariappan N, Elks CM, Haque M, Soltani Z, Reisin E, and Francis J (2009) Effects of pyrrolidine dithiocarbamate on high-fat diet-induced metabolic and renal alterations in rats. *Life Sci* **85**: 357-364.

Foster KG and Fingar DC (2010) Mammalian target of rapamycin (mTOR): conducting the cellular signaling symphony. *J Biol Chem* **285**: 14071-14077.

He HJ, Zhu TN, Xie Y, Fan J, Kole S, Saxena S, and Bernier M (2006) Pyrrolidine dithiocarbamate inhibits interleukin-6 signaling through impaired STAT3 activation and association with

transcriptional coactivators in hepatocytes. *J Biol Chem* **281**: 31369-31379.

Horak P, Crawford AR, Vadysirisack DD, Nash ZM, DeYoung MP, Sgroi D, and Ellisen LW (2010) Negative feedback control of HIF-1 through REDD1-regulated ROS suppresses tumorigenesis. *Proc Natl Acad Sci U S A* **107**: 4675-4680.

Huang J, Kaminski PM, Edwards JG, Yeh A, Wolin MS, Frishman WH, Gewitz MH, and Mathew R (2008) Pyrrolidine dithiocarbamate restores endothelial cell membrane integrity and attenuates monocrotaline-induced pulmonary artery hypertension. *Am J Physiol Lung Cell Mol Physiol* **294**: L1250-L1259.

Hwang-Verslues WW, Chang PH, Wei PC, Yang CY, Huang CK, Kuo WH, Shew JY, Chang KJ, Lee EY, and Lee WH (2011) miR-495 is upregulated by E12/E47 in breast cancer stem cells, and promotes oncogenesis and hypoxia resistance via downregulation of E-cadherin and REDD1. *Oncogene* **30**: 2463-2474.

Jastrzebski K, Hannan KM, Tchoubrieva EB, Hannan RD, and Pearson RB (2007) Coordinate regulation of ribosome biogenesis and function by the ribosomal protein S6 kinase, a key mediator of mTOR function. *Growth Factors* **25**: 209-226.

Jin HO, Seo SK, Woo SH, Kim ES, Lee HC, Yoo DH, An S, Choe TB, Lee SJ, Hong SI, Rhee CH, Kim JI, and Park IC (2009) Activating transcription factor 4 and CCAAT/enhancer-binding protein-beta negatively regulate the mammalian target of rapamycin via Redd1 expression in response to oxidative and endoplasmic reticulum stress. *Free Radic Biol Med* **46**: 1158-1167.

Kim SY and Volsky DJ (2005) PAGE: parametric analysis of gene set enrichment. *BMC Bioinformatics* **6**: 144.

Komar AA, and Hatzoglou M (2011) Cellular IRES-mediated translation: the war of ITAFs in pathophysiological states. *Cell Cycle* **10**: 229-240.

Kuehn HS, Jung MY, Beaven MA, Metcalfe DD, and Gilfillan AM (2011) Prostaglandin E2 activates and utilizes mTORC2 as a central signaling locus for the regulation of mast cell chemotaxis and mediator release. *J Biol Chem* **286**: 391-402.

Lee DF, Kuo HP, Chen CT, Hsu JM, Chou CK, Wei Y, Sun HL, Li LY, Ping B, Huang WC, He X, Hung JY, Lai CC, Ding Q, Su JL, Yang JY, Sahin AA, Hortobagyi GN, Tsai FJ, Tsai CH, and Hung MC (2007) IKKβ suppression of TSC1 links inflammation and tumor angiogenesis via the mTOR pathway. *Cell* **130**: 440-455.

Lin L, Stringfield TM, Shi X, and Chen Y (2005) Arsenite induces a cell stress-response gene, RTP801, through reactive oxygen species and transcription factors Elk-1 and CCAAT/enhancer-binding protein. *Biochem J* **392:** 93-102.

Liu SF, Ye X, and Malik AB (1999) Inhibition of NF-κB activation by pyrrolidine dithiocarbamate prevents in vivo expression of proinflammatory genes. *Circulation* **100**: 1330–1337.

Ma L, Chen Z, Erdjument-Bromage H, Tempst P, and Pandolfi PP (2005) Phosphorylation and functional inactivation of TSC2 by Erk implications for tuberous sclerosis and cancer pathogenesis. *Cell* **121**: 179–193.

Maedler K, Sergeev P, Ris F, Oberholzer J, Joller-Jemelka HI, Spinas GA, Kaiser N, Halban PA, and Donath MY (2002) Glucose-induced beta cell production of IL-1beta contributes to glucotoxicity in human pancreatic islets. *J Clin Invest* **110**: 851-860.

Malm TM, Iivonen H, Goldsteins G, Keksa-Goldsteine V, Ahtoniemi T, Kanninen K, Salminen A, Auriola S, Van Groen T, Tanila H, and Koistinaho J (2007) Pyrrolidine dithiocarbamate activates Akt and improves spatial learning in APP/PS1 mice without affecting beta-amyloid burden. *J Neurosci* **27**: 3712-3721.

Mayer C and Grummt I (2006) Ribosome biogenesis and cell growth: mTOR coordinates transcription by all three classes of nuclear RNA polymerases. *Oncogene* **25**: 6384-6391.

Meng F, Henson R, Wehbe-Janek H, Smith H, Ueno Y, and Patel T (2007) The MicroRNA let-7a modulates interleukin-6-dependent STAT-3 survival signaling in malignant human cholangiocytes. *J Biol Chem* **282**: 8256-8264.

Nai YJ, Jiang ZW, Wang ZM, Li N, and Li JS (2007) Prevention of cancer cachexia by pyrrolidine

dithiocarbamate (PDTC) in colon 26 tumor-bearing mice. *JPEN J Parenter Enteral Nutr* **31**: 18-25.

Neurath MF and Finotto S (2011) IL-6 signaling in autoimmunity, chronic inflammation and inflammation-associated cancer. *Cytokine Growth Factor Rev* **22**: 83-89.

Nurmi A, Goldsteins G, Närväinen J, Pihlaja R, Ahtoniemi T, Gröhn O, and Koistinaho J (2006) Antioxidant pyrrolidine dithiocarbamate activates Akt-GSK signaling and is neuroprotective in neonatal hypoxia-ischemia. *Free Radic Biol Med* **40**: 1776-1784.

Pineau P, Volinia S, McJunkin K, Marchio A, Battiston C, Terris B, Mazzaferro V, Lowe SW, Croce CM, and Dejean A (2010) miR-221 overexpression contributes to liver tumorigenesis. *Proc Natl Acad Sci U S A* **107**: 264-269.

Ramanathan A and Schreiber SL (2009) Direct control of mitochondrial function by mTOR. *Proc Natl Acad Sci U S A* **106**: 22229-22232.

Sarbassov DD, Guertin DA, Ali SM, and Sabatini DM (2005) Phosphorylation and regulation of Akt/PKB by the rictor-mTOR complex. *Science* **307**: 1098-1101.

Schreck R, Meier B, Männel DN, Dröge W, and Baeuerle PA (1992) Dithiocarbamates as potent inhibitors of nuclear factor kappa B activation in intact cells. *J Exp Med* **175**: 1181-1194.

Shoshani T, Faerman A, Mett I, Zelin E, Tenne T, Gorodin S, Moshel Y, Elbaz S, Budanov A, Chajut A, Kalinski H, Kamer I, Rozen A, Mor O, Keshet E, Leshkowitz D, Einat P, Skaliter R, and Feinstein E (2002) Identification of a novel hypoxia-inducible factor 1–responsive gene, RTP801, involved in apoptosis. *Mol Cell Biol* **22**: 2283–2293.

Sofer A, Lei K, Johannessen CM, and Ellisen LW (2005) Regulation of mTOR and cell growth in response to energy stress by REDD1. *Mol Cell Biol* **25**: 5834-5845.

Song S, Kole S, Precht P, Pazin MJ, and Bernier M (2010) Activation of heat shock factor 1 plays a role in pyrrolidine dithiocarbamate-mediated expression of the co-chaperone BAG3. *Int J Biochem Cell Biol* **42**: 1856-1863.

Tian XF, Yao JH, Li YH, Gao HF, Wang ZZ, Yang CM, and Zheng SS. (2006) Protective effect of pyrrolidine dithiocarbamate on liver injury induced by intestinal ischemia-reperfusion in rats.

Hepatobiliary Pancreat Dis Int **5**: 90-95.

Tusher VG, Tibshirani R, and Chu G (2001) Significance analysis of microarrays applied to the ionizing radiation response. *Proc Natl Acad Sci USA* **98**: 5116-5121.

Wang Y, Xie Y, Bernier M, and Wainer IW (2009) Determination of free and protein-bound glutathione in HepG2 cells using capillary electrophoresis with laser-induced fluorescence detection. *J Chromatogr A* **1216**: 3533-3537.

Wullschleger S, Loewith R, and Hall MN (2006) TOR signaling in growth and metabolism. *Cell* **124**: 471-484.

Xie Y, Kole S, Precht P, Pazin MJ, and Bernier M (2009) S-glutathionylation impairs signal transducer and activator of transcription 3 activation and signaling. *Endocrinology* **150**: 1122-1131.

Footnotes

This research was supported entirely by the Intramural Research Program of the NIH, National Institute on Aging.

JPET Fast Forward. Published on September 13, 2011 as DOI: 10.1124/jpet.111.185678
This article has not been copyedited and formatted. The final version may differ from this version.

Figure Legends

Fig. 1. Effects of PDTC and IL-6 on the regulation of DDIT4 mRNA and protein. A, Temporal expression of the DDIT4 gene in HepG2 cells treated with PDTC (●) or IL-6 (❍). Data were obtained from the microarray analysis. B, Serum-starved HepG2 cells were left alone or pretreated with actinomycin D (Act. D, 1 μg/ml) for 1 h followed by the addition of PDTC (50 μM) or IL-6 (20 ng/ml) for 30 min and 1 h. Total RNA was extracted and then analyzed by real-time PCR. Data are presented as fold increase relative to the untreated group. Bars represent the average ± S.D. of two independent experiments, each performed in triplicate dishes. **, $P < 0.01$, ***, $P < 0.001$ vs. untreated controls. C, Cells were serum-starved and then treated with either PDTC, IL-6 or the combination 'PDTC+IL-6' for 1h to 4 h. Cell lysates were prepared and Western blot analysis was performed using primary antibodies raised against DDIT4, and total and tyrosine phosphorylated STAT3 (pY-STAT3). STAT3 was included as a loading control. Data are representative of at least three independent experiments. Graphical representation of DDIT4 and pY-STAT3 blots is shown (*lower panels*). D, Serum-starved HepG2 cells were incubated with vehicle, PDTC for 3 h or IL-6 for 1-6 h. Representative immunoblots of DDIT4, pY-STAT3 and that of the loading control, Hsp90α, are shown.

Fig. 2. PDTC blocked IL-6-induced increase in mTORC1 function. Serum-starved HepG2 cells were treated either with PDTC, IL-6 or the combination PDTC+IL-6 for the indicated periods of time. Cell lysates were prepared and Western blot analysis was performed, looking at the phosphorylation of mTORC1 downstream targets, S6K1 (T389) and 4EBP1 (T37/46), as well as that of Akt (T308 and S473) and its direct targets, GSK3β (S9) and TSC2 (T1462). STAT3 was included as a loading control. Similar results were obtained in two other separate experiments.

Fig. 3. Effect of DDIT4 gene knockdown on mTORC1 function. HepG2 cells were transfected with the negative control siRNA (filled bars) or *DDIT4* siRNA (hatched bars) for 48 h. Cells were serum-starved and then treated with PDTC, IL-6, or the combination PDTC+IL-6 for 2 h. Lysates were immunoblotted with the indicated primary antibodies using β-tubulin as a loading control. Quantitative analysis of the immunoblots is shown and normalized to the PDTC signal (DDIT4) or vehicle-treated group (pS6K1 and p4E-BP1) from cells transfected with the nonsilencing siRNA. Similar results were obtained in a second independent experiment. The migration of molecular mass markers (values in kilodaltons) is shown on the left of immunoblots.

Fig. 4. Effects of PDTC and IL-6 on global protein translation. A, Administration of the negative control siRNA or DDIT4 siRNA was performed for 48 h in HepG2 cells, after which cells were serum-starved and then incubated with vehicle, rapamycin (20 nM), PDTC, PDTC + rapamycin, or IL-6 for 2 h. After washing, cells were incubated in Met/Cys-free medium for 30 min followed by [^{35}S]-Met/Cys labeling for 15 min. Cell lysates were resolved by SDS-polyacrylamide gel electrophoresis, transferred onto PVDF membrane and autoradiography was performed. The membrane was probed with anti-β−actin antibody to confirm equal protein load in each lane. This experiment was repeated twice with comparable results. *, denotes increased translation in response to PDTC. B, Serum-starved HepG2 cells were incubated in the absence (-) or the presence (+) of rapamycin (20 nM) for 1 h followed by the addition of IL-6 or insulin (100 nM) for 30 min. Cell lysates were immunoblotted with antibodies against phosphorylated (T389) and total S6K1. *Rel. Units*, the ratios of phospho/total S6K1 are shown relative to vehicle-treated controls. Similar results were obtained in a second independent experiment.

JPET Fast Forward. Published on September 13, 2011 as DOI: 10.1124/jpet.111.185678
This article has not been copyedited and formatted. The final version may differ from this version.

Table 1. Number of gene sets affected by PDTC and IL-6 in HepG2 cells

	PDTC			IL-6		
Time (h)	Total	Up (%)	Down (%)	Total	Up (%)	Down (%)
1	61	21 (34.4)	40 (65.6)	57	46 (80.7)	11 (19.3)
2	66	30 (45.5)	36 (54.5)	103	69 (67.0)	34 (33.0)
4	95	44 (46.3)	51 (53.7)	104	69 (66.3)	35 (33.7)
8	104	54 (51.9)	50 (48.1)	102	73 (71.6)	29 (28.4)

All gene sets were significant at $P < 0.05$.

JPET Fast Forward. Published on September 13, 2011 as DOI: 10.1124/jpet.111.185678
This article has not been copyedited and formatted. The final version may differ from this version.

Table 2. List of shared gene sets after 8-h treatment with PDTC and IL-6 in HepG2 cells

		PDTC		IL-6	
Size	Name	z-score	rank	z-score	rank
95	breast_cancer_estrogen_signalling	6.09	1	-2.67	96
105	LEU_UP	4.65	2	2.78	37
138	GPCRs_Class_A_Rhodopsin-like	3.28	9	-3.70	99
28	nktPathway	2.67	11	-2.59	93
28	inflamPathway	2.67	12	-1.97	89
15	stemPathway	2.59	13	-1.89	87
17	th1th2Pathway	2.47	14	-2.33	91
21	cytokinePathway	1.98	16	-2.64	95
131	cell_surface_receptor_linked_signal_transduction	1.90	18	-3.00	98
23	GPCRs_Class_B_Secretin-like	1.25	31	-1.44	85
10	il5Pathway	1.00	35	-1.22	84
8	asbcellPathway	0.95	36	-0.77	75
15	tall1Pathway	0.88	37	-0.89	78
4	slrp2Pathway	0.65	49	-1.05	79
6	neurotransmittersPathway	0.61	51	-1.75	86
3	aifPathway	-1.55	59	1.83	65
6	CR_TRANSPORT	-1.58	60	1.31	71
15	MAP00510_N_Glycans_biosynthesis	-1.61	61	3.37	23
7	KET	-1.75	62	1.57	68
22	MAP00500_Starch_and_sucrose_metabolism	-2.10	66	2.93	35
15	TCA	-2.11	67	2.05	60

JPET Fast Forward. Published on September 13, 2011 as DOI: 10.1124/jpet.111.185678
This article has not been copyedited and formatted. The final version may differ from this version.

20	MAP00650_Butanoate_metabolism	-2.47	72	3.93	13
37	CR_REPAIR	-2.47	73	2.75	38
18	MAP00020_Citrate_cycle_TCA_cycle	-2.79	80	3.15	28
3	torPathway	-2.99	83	1.22	72
49	mRNA_splicing	-3.08	84	4.12	10
28	Krebs-TCA_Cycle	-3.22	88	2.63	42
19	GLYCOGEN	-3.38	90	3.09	30
42	mRNA_processing	-3.48	92	3.09	31
7	MAP00720_Reductive_carboxylate_cycle (CO_2 fixation)	-4.04	96	3.25	25
21	MAP00120_Bile_acid_biosynthesis	-4.05	97	3.55	17
10	MAP00100_Sterol_biosynthesis	-4.11	98	3.16	27
19	MAP00640_Propanoate_metabolism	-4.50	100	4.27	8
24	MAP00280_Valine_leucine_and_isoleucine degradation	-5.61	102	7.44	4
393	Human_mitoDB_6_2002	-6.56	103	3.07	32
404	Mitochondr	-7.46	104	3.53	20

Size indicates the number of genes in each gene set. A brief description of each gene set is summarized in Supplemental Table 3. All gene sets were significant at $P < 0.05$.

JPET Fast Forward. Published on September 13, 2011 as DOI: 10.1124/jpet.111.185678
This article has not been copyedited and formatted. The final version may differ from this version.

Table 3. Partial list of ribosomal protein genes whose expression is reciprocally regulated by a 2-h treatment with PDTC and IL-6 in HepG2 cells

			PDTC	IL-6
Accession	Symbol	Gene Name	zratio	zratio
NM_001003.2	RPLP1	Ribosomal protein, large, P1	9.232	-5.024
NM_003973.2	RPL14	Ribosomal protein L14	4.409	-4.296
NM_000978.2	RPL23	Ribosomal protein L23	2.684	-9.910
NM_000988.2	RPL27	Ribosomal protein L27	1.204	-7.297
NM_001020.4	RPS16	Ribosomal protein S16	3.328	-7.474
NM_001005.3	RPS3	Ribosomal protein S3	2.543	-7.059
NM_001031.4	RPS28	Ribosomal protein S28	2.435	-6.941
NM_001030009.1	RPS15A	Ribosomal protein S15a	1.216	-8.458

All genes were significant at $P < 0.05$ when compared to untreated controls. A complete list of ribosomal protein genes can be found in Supplemental Table 5.

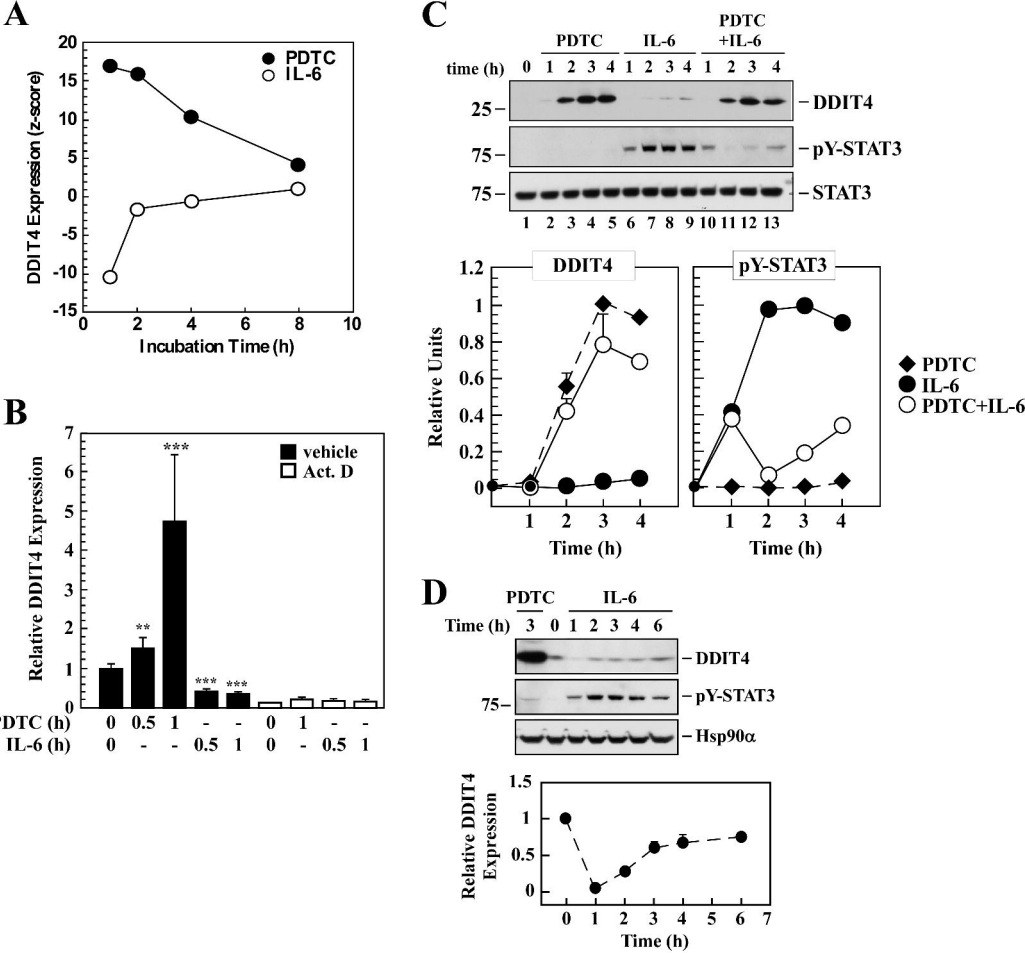

Song et al., Fig. 1

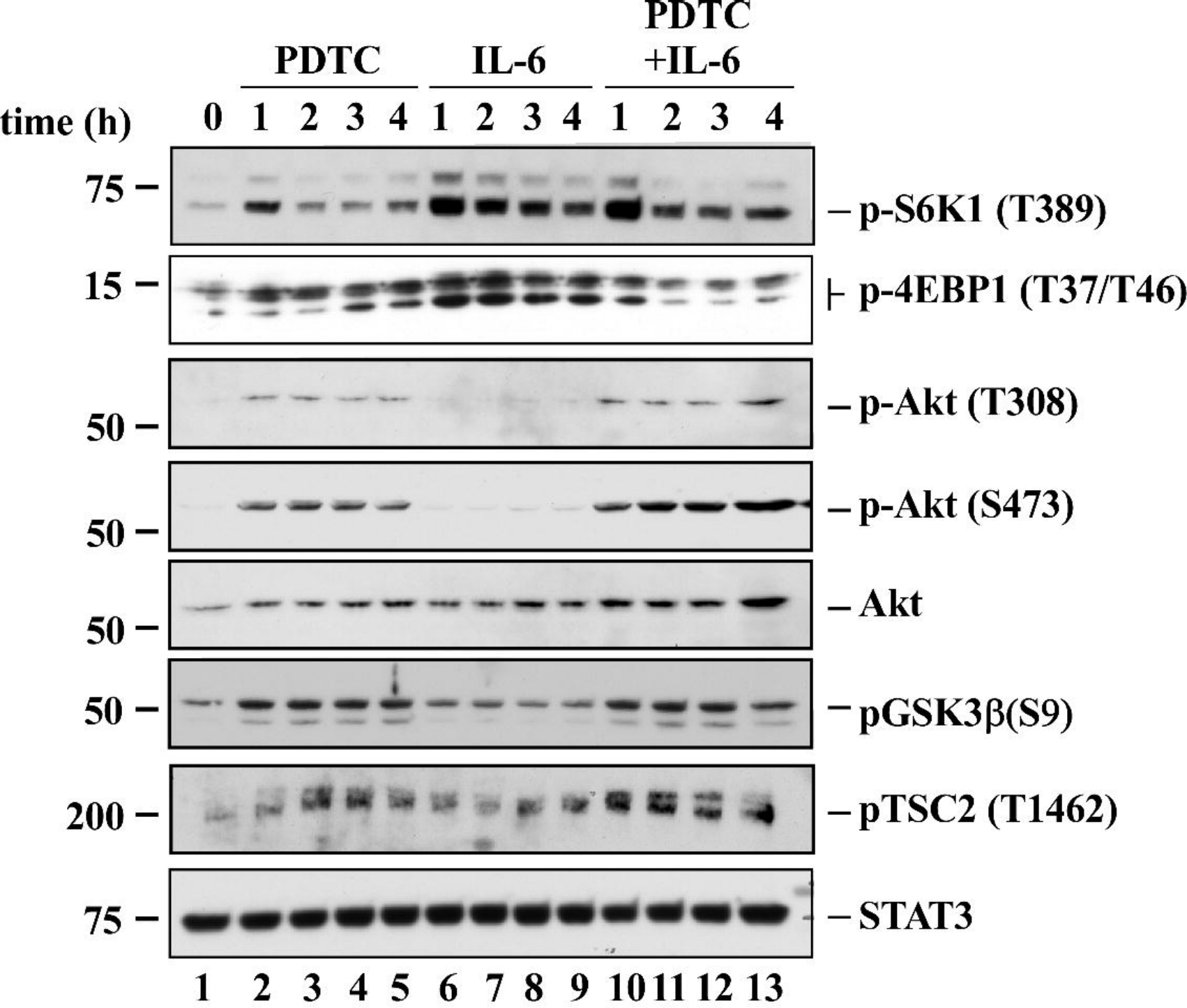

Song et al., Fig. 2

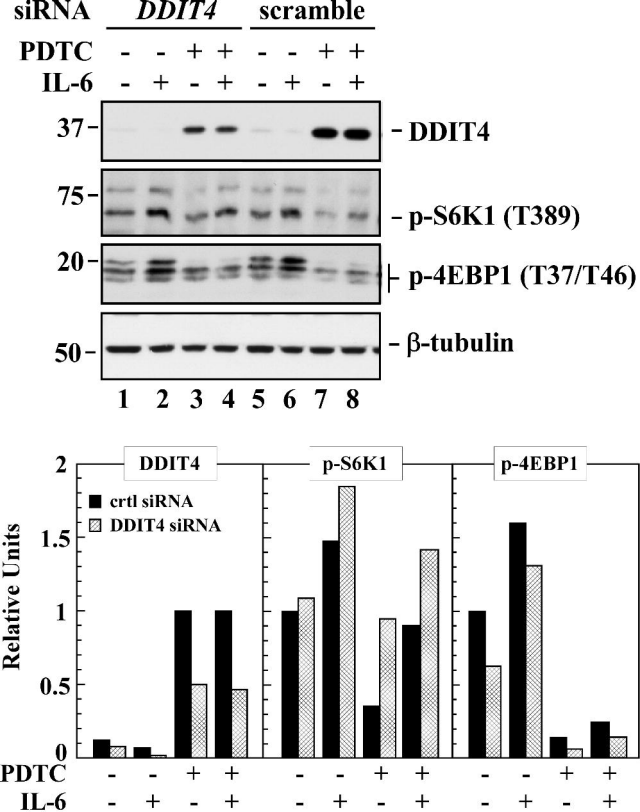

Song et al., Fig. 3

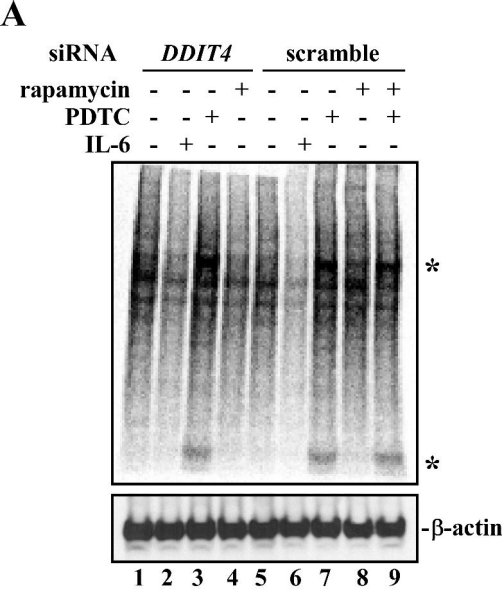

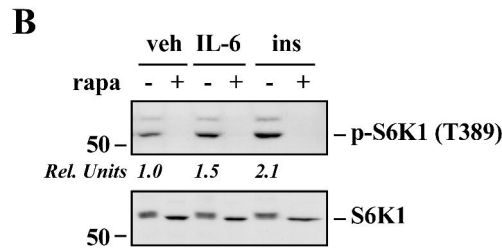

Song et al., Fig. 4